Molecular Tracing of Riverine Soil Organic Matter From the Central Himalaya

L. Märki, M. Lupker, A. Gajurel, H. Gies, N. Haghipour, S. Gallen, C. France-Lanord, J. Lavé, T. Eglinton

Geophysical Research Letters

RESEARCH LETTER
10.1029/2020GL087403

Molecular Tracing of Riverine Soil Organic Matter From the Central Himalaya

L. Märki[1], M. Lupker[1], A. P. Gajurel[2], H. Gies[1], N. Haghipour[1,3], S. Gallen[4], C. France-Lanord[5], J. Lavé[5], and T. Eglinton[1]

[1]Geological Institute, ETH Zürich, Zürich, Switzerland, [2]Department of Geology, Tribhuvan University, Kathmandu, Nepal, [3]Ion Beam Physics, ETH Zürich, Zürich, Switzerland, [4]Department of Geosciences, Colorado State University, Fort Collins, CO, USA, [5]Centre de Recherches Pétrographiques et Géochimiques (CRPG), CNRS–Université de Lorraine, Vandœuvre-lès-Nancy, France

Key Points:
- A calibration for soil branched glycerol dialkyl glycerol tetraether (brGDGT) signals against an elevation profile is developed
- The provenance of soil organic matter in riverine suspended sediments is traced based on corresponding brGDGT distributions
- Soil organic carbon in most river sediments originates from the entire soil-covered catchment, indicating uniform soil organic matter export

Supporting Information:
- Supporting Information S1
- Table S1
- Table S2
- Table S3

Correspondence to:
L. Märki,
lena.maerki@erdw.ethz.ch

Citation:
Märki, L., Lupker, M., Gajurel, A. P., Gies, H., Haghipour, N., Gallen, S., et al. (2020). Molecular tracing of riverine soil organic matter from the Central Himalaya. *Geophysical Research Letters*, *47*, e2020GL087403. https://doi.org/10.1029/2020GL087403

Received 7 FEB 2020
Accepted 2 AUG 2020
Accepted article online 10 AUG 2020

Abstract The isomer distribution of branched glycerol dialkyl glycerol tetraethers (brGDGTs) in soils has been shown to correlate to the local mean annual temperature. Here, we explore the use of brGDGT distributions as proxy for the elevation at which soil organic carbon is preferentially mobilized in the Central Himalaya. Soil brGDGT distributions collected along an altitudinal profile, spanning elevations from 200 to 4,450 m asl, are linearly correlated to elevation. We use this calibration to trace the provenance of soil organic matter in suspended sediments of rivers draining the Himalaya. BrGDGT distributions of fluvial sediments reflect the mean elevation of the soil cover in most catchments. Inverse modeling of the brGDGT data set suggests similar relative contribution to soil organic carbon mobilization from different land covers within a factor 2. We conclude that riverine soil organic carbon export in the Himalaya mostly occurs pervasively and is at the catchment scale insensitive to anthropogenic perturbations.

Plain Language Summary Soil degradation influences the global climate and has direct impacts on the ability of soils to deliver economic and ecological services. Identifying the source of eroded soil-derived carbon entrained in sediments of large rivers remains challenging. In this contribution, we use the temperature-sensitive signature of soil microbe-derived organic molecules to trace the source of soil carbon exported in river sediments of the rapidly eroding Central Himalaya of Nepal. Molecular signatures of soils, sampled over a wide range of elevations, and hence temperatures are plotted on an elevation profile. River sediments are then compared to soil signatures in order to identify elevations of preferential soil export through rivers. Our data shows that soil-derived carbon is sampled uniformly over most of the catchments, indicating that soil export by Himalayan rivers is not driven by localized human perturbations such as agriculture or deforestation.

1. Introduction

Soils represent the largest organic carbon (OC) reservoir exposed at the Earth's surface (Jobbagy & Jackson, 2000). The exchange of soil OC (SOC) with other carbon reservoirs such as the atmosphere or the geosphere exerts fundamental controls on the carbon budget of the Earth's surface on time scales ranging from decades to millions of years. Nevertheless, SOC dynamics, especially the lateral mobilization of carbon associated to soil erosion, remains one of the least constrained components of the carbon cycle (Doetterl et al., 2016).

On time scales of decades to millennia, soil erosion is an important process that redistributes OC across the landscape (e.g., Doetterl et al., 2016; Yue et al., 2016) and exerts a primary control on SOC stocks (Patton et al., 2019; Yoo et al., 2006). The overall carbon budget of soil erosion on short time scales remains a subject of debate (Stockmann et al., 2013). It may act either as a carbon source with respect to atmospheric CO_2 due to degradation and mineralization of SOC exposed during erosion (Jacinthe & Lal, 2001; Schlesinger, 1995) or as a carbon sink through effective OC sequestration and stabilization for instance in sediment accumulating areas (Berhe et al., 2012; Smith et al., 2001; Stallard, 1998). These considerations are particularly relevant in light of increasing anthropogenic pressure on soil systems that have led to up to a 2 orders of magnitude increase in soil erosion rates (Montgomery, 2007) and represent a significant perturbation of the modern carbon cycle (Wang et al., 2017).

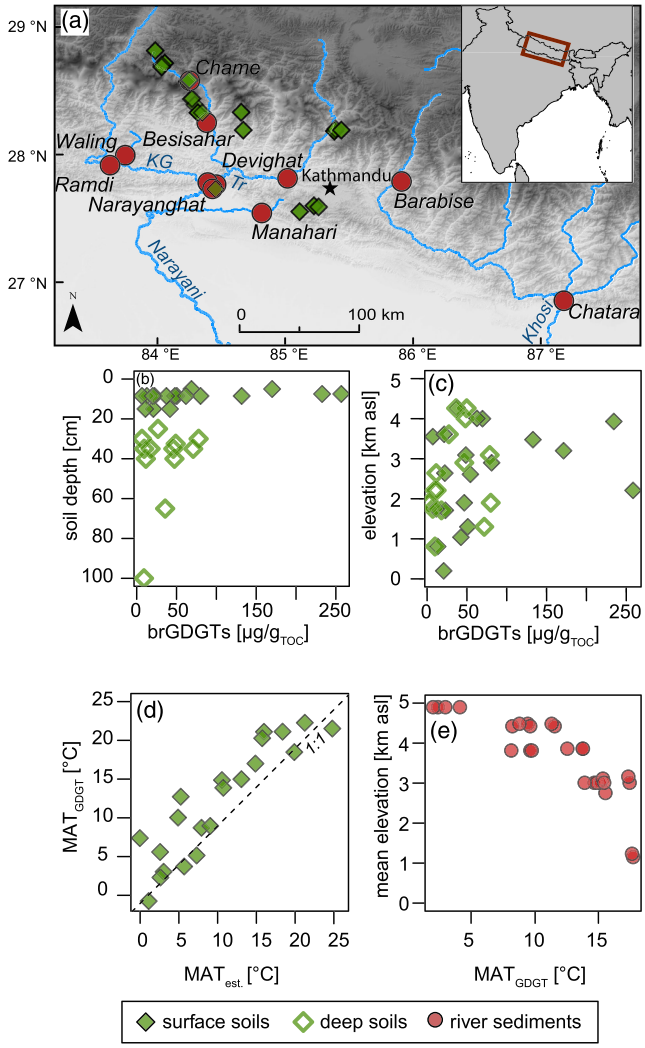

Figure 1. (a) Map of the Central Himalaya (Nepal) displaying the soil (diamonds) and river (circles) sampling sites. Close to the station in Narayanghat, three rivers were sampled: the Khali Gandaki (KG), the Trisuli (Tr), and the Narayani. (b) Soil brGDGT concentrations normalized to the TOC content of soil samples as a function of the mean sampling depth. (c) Soil brGDGT concentrations normalized to the TOC content as a function of the elevation. (d) Estimated MAT values ($MAT_{est.}$) for sampling locations as a function of MAT calculated from soil brGDGTs (MAT_{GDGT}). (e) MAT_{GDGT} calculated with river sediment brGDGTs as a function of the mean catchment elevation.

On geological timescales (millions of years), the erosion of SOC and its transport by rivers can also act as a long-term carbon sink since a fraction of the riverine particulate OC is buried on continental margins (e.g., France-Lanord & Derry, 1997; Ludwig et al., 1996).

Although SOC stocks in mountain regions account for a small, yet poorly quantified, fraction of global SOC stocks (Scharlemann et al., 2014), these rapidly eroding landscapes contribute disproportionally to the total export of OC (Galy et al., 2015). Mountain ecosystems are also particularly vulnerable to soil erosion and associated changes in SOC stocks through changes in land use or climate (e.g., Alewell et al., 2008). Despite the importance of soil erosion processes in mountain landscapes for global carbon budgets, few approaches are available to quantify and fingerprint soil erosion and associated SOC export, especially at the larger catchment scale.

Soil loss induced by deforestation and agriculture, particularly in steep mountain regions such as the Himalaya, has received much attention (e.g., Eckholm, 1975; Semwal et al., 2004; Wasson et al., 2008). Recent studies show that traditional terracing practices probably have a minor effect on soil erosion but that modern agricultural methods and managed forests contribute more importantly to anthropogenic soil loss (Gardner & Gerrard, 2003; Upadhayay et al., 2018). Anthropogenic perturbations of soil erosion in the Himalayan region could also be overshadowed by natural active denudation processes such as frequent mass wasting in the steeper areas (Hoffmann et al., 2016; West et al., 2015).

In this study, we use the distributions of branched glycerol dialkyl glycerol tetraethers (brGDGTs) in soils and river sediments from 11 nested catchments (367–57,700 km^2) in the Central Himalaya of Nepal to constrain the dominant elevations of SOC mobilization and hence the provenance of soils eroded from a steep mountainous environment. BrGDGTs are a suite of lipids produced by microbes that occur ubiquitously in soils (Schouten et al., 2013; Weijers et al., 2007). The relative abundance of different brGDGT isomers (here referred to as brGDGT distributions) depends on environmental parameters such as mean annual temperature (MAT) and soil pH (Weijers, Schouten, et al., 2007), which makes them useful paleo-climate proxies (e.g., Sinninghe Damasté et al., 2012; Weijers et al., 2007). Despite evidence for in situ brGDGTs production in some aqueous environments (e.g., De Jonge et al., 2014), it has recently been shown that brGDGT signatures in suspended sediments can be used for tracing SOC inputs in riverine systems (Kirkels et al., 2020). Here, we use the MAT calculated from brGDGT isomer distributions as a proxy for the elevation from which SOC is mobilized and entrained in riverine suspended sediments of the Central Himalaya.

2. Materials and Methods

2.1. Study Area and Sampling

Rivers draining the Central Himalaya integrate a broad diversity of environmental conditions, with elevations ranging from over 8,000 m in the central part of the range to ~150 m upon entering the Indo-Gangetic floodplain. The precipitation regime of the Central Himalaya is strongly influenced by the Indian Summer Monsoon, and a sharp precipitation gradient from the wetter Middle Hills to the dryer Upper Himalaya characterizes the region (Burbank et al., 2003). The steep valleys of the Upper Himalaya,

where mass wasting is the principal agent of erosion (Marc et al., 2019), are characterized by high erosion rates (0.5–2 mm/yr) (Gabet et al., 2008). The land cover of the Upper Himalaya consists mainly of natural forests, shrubland and bare land, or glaciers, whereas the Middle Hills are mostly covered by forests or agricultural land, such as rice paddies.

Samples for this study consisted of both soil samples, used to calibrate the brGDGT-calculated MAT against elevation, and river suspended sediment samples, which are used to identify the provenance of soil organic matter eroded from their respective catchments. Sample locations are shown in Figure 1a, and full details are reported in Tables S2 and S3 in the supporting information. Soils samples ($n = 38$) were collected over several field campaigns from 2009 to 2017. The sampling locations cover a variety of conditions such as elevation, annual precipitation, and aspect. At each location, soil samples were taken at depth intervals below the surface, if possible, down to bedrock. River sediments ($n = 28$) were sampled from rivers draining catchments encompassing the soil sampling locations between 2015 and 2017. These consisted of two sample types: (i) river samples, sampled during monsoon in 2017, by sampling surface river water followed by pressure filtration through 0.2 μm PES membranes; and (ii) integrated river sediments that represent an average composition of sediments over 2-week periods (for detailed sampling description, see the supporting information). No difference was found in GDGT compositions of sediments sampled using either method. Both types of suspended sediment samples are collected from surface river water and are taken to be representative of the entire water column as previous studies did not find any systematic variation of brGDGT signals with depth (Freymond et al., 2018; Kirkels et al., 2020). Some samples have been taken shortly after the 2015 Gorkha earthquake which triggered a large number of landslides in parts of the Central Himalaya (Roback et al., 2018).

2.2. BrGDGTs and TOC Measurements

Soils and river sediments were frozen and freeze-dried at ETH Zürich. Soils were sieved, and the fraction <2 mm was used for further analysis. Analytical techniques for brGDGT analyses follow Hopmans et al. (2016) and Freymond et al. (2017) and are summarized here with a detailed description in the supporting information. Briefly, between 2 and 3 g of the soil samples and around 20 g of the river sediments were extracted with solvents in a microwave or an automated extraction system. After purification via column chromatography and prefiltration, the GDGT distributions were analyzed by high-performance liquid chromatography-mass spectrometry (HPLC-MS) at ETH Zürich. Absolute concentrations of GDGTs were determined by the addition of an internal standard (Huguet et al., 2006). The relative abundance of the different GDGT isomers was determined based on integrated peak areas of mass chromatograms. The resulting brGDGT distributions are then used to calculate the corresponding MAT following the empirical calibration established by De Jonge et al. (2014) (for more details on GDGT temperature calibrations, see the supporting information).

The total OC (TOC) content of all samples was measured with an elemental analyzer at ETH Zurich (see the supporting information).

2.3. Climate and Remote Sensing Data Sets

In order to quantify soil cover in the studied catchments, land cover maps from the International Centre for Integrated Mountain Development (Uddin et al., 2015) and from the National Geomatics Center of China (Jun et al., 2014) were used. Normalized difference vegetation index (NDVI) maps (MOD13Q1v006) were derived from NASA's MODIS project (Didan, 2015). The mean elevations of soils and of vegetated areas in a catchment were calculated with the above-mentioned data sets using standard GIS software. The MAT corresponding to land covers and sampling points was calculated using a linear regression between elevation and MAT inferred from temperature data of local weather stations (HMG, 1995; Putkonen, 2004) (see also the supporting information). Precipitation data are taken from NASA's GIOVANNI platform.

3. Results

3.1. BrGDGT Signatures in Himalayan Soils

The mean absolute concentration of brGDGTs, determined as a composite of all branched isomers, in the soil samples is 3.3 $\mu g/g_{soil}$ (range: 0.005–17.9 $\mu g/g_{soil}$) resulting in mean TOC-normalized brGDGT concentrations of 53.4 $\mu g/g_{TOC}$ (2–259 $\mu g/g_{TOC}$) (Table S2). While absolute brGDGT concentrations decrease with

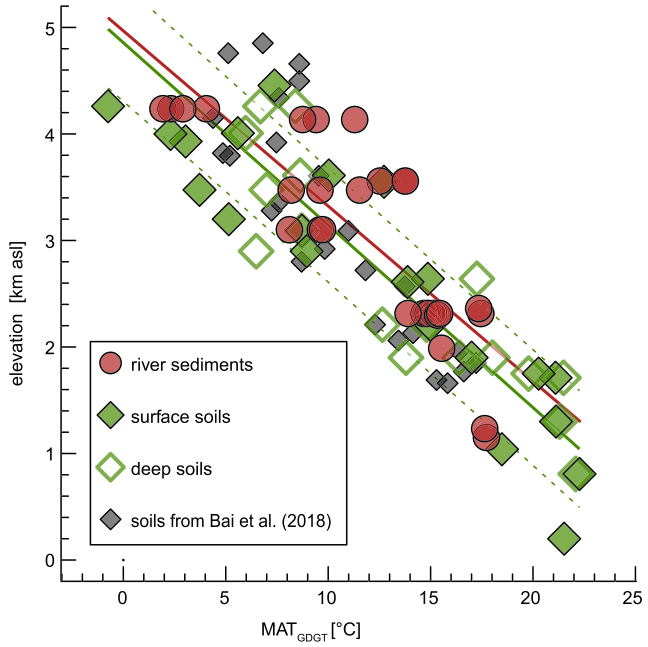

Figure 2. MAT_{GDGT} calculated of brGDGTs in soils (green diamonds, this study; gray diamonds, nearby soil samples reported in Bai et al., 2018) and in river sediments (circles) as a function of elevation. The elevation depicted for river sediments corresponds to the mean elevation of the soil-covered areas of their respective catchments. Green lines show the linear regression ($r^2 = 0.81$) through the MAT_{GDGT} of all the soils and the one-sigma confidence interval; the red line shows the linear regression through MAT_{GDGT} of river sediments.

soil depth, a clear trend is not visible for TOC-normalized brGDGT concentrations (Figure 1b). Both absolute and normalized brGDGT concentrations do not show any significant relationship with the soil elevation, as found in previous studies (Deng et al., 2016; Ernst et al., 2013; Kirkels et al., 2020) (Figure 1c). Environmental parameters such as the measured MAT, the total annual precipitation, and the aspect of the sampling site are also unrelated to brGDGT concentrations in Himalayan soils (Figure S2).

The MAT reconstruction calculated from brGDGT distributions of surface soils (MAT_{GDGT}) is in good agreement with the temperature estimated from climate data ($MAT_{est.}$, Figure 1d) ($r^2 = 0.82$, $p < 0.05$, RMSE = 3.0°C). The MAT_{GDGT} values of all soils also show a robust negative linear correlation to elevation (Figure 2) ($r^2 = 0.81$, $p < 0.05$). There is no significant difference between the MAT_{GDGT}-elevation correlation for surface and deep soils. Our soil data agree well with temperature estimated from nearby soils reported in Bai et al. (2018) (Figure 2).

3.2. BrGDGT Signatures in Suspended River Sediments

TOC-normalized brGDGT concentrations of suspended river sediments lie between 0.25 and 28 $\mu g/g_{TOC}$ (mean: 8.9 $\mu g/g_{TOC}$) (Table S3). A general downstream increase in TOC-normalized brGDGT concentrations of suspended sediments can be observed despite large scatter. No systematic trend in brGDGT concentrations during the monsoon season or between sampling years is evident (Figure S3). Reconstructed MAT_{GDGT} values vary between 1.9°C and 17.7°C. Figure 1e shows that the MAT_{GDGT} correlates with the mean elevation of sampled river catchments ($r^2 = 0.71$, $p < 0.05$).

4. Discussion

4.1. MAT Reconstruction With Soil brGDGTs

The calculated MAT_{GDGT} from surface soils in the Central Himalaya agree with the estimated temperatures at the sampling locations (Figure 1d). This suggests that the global calibration for temperature reconstruction with brGDGT distributions from De Jonge, Hopmans, et al. (2014) is applicable in the Himalaya. Several studies have shown that brGDGT-based indices are correlated with adiabatic temperature change along elevation profiles in different regions worldwide (e.g., Bai et al., 2018; Deng et al., 2016; Ernst et al., 2013; Peterse et al., 2009). This agrees with the calculated MAT_{GDGT} of Himalayan soils which strongly correlates with elevation (Figure 2). The obtained lapse rate (6.5°C/km) is similar to the estimated lapse rate for the Central Himalaya (5.3°C/km, Putkonen, 2004). Soil brGDGT signals likely integrate environmental conditions over a time scale of at least decades, rendering them insensitive to seasonal or interannual climatic variabilities (Cao et al., 2018).

4.2. Origin of the brGDGT Signal in River Sediments

The strong correlation between the calculated MAT_{GDGT} and soil elevation (Figure 2) provides an opportunity to trace the sources and inputs of soil organic matter exported by the fluvial system and to refine our understanding of soil mobilization processes in rapidly eroding landscapes. Such an assessment is based on the assumptions that (i) the studied proxy is distributed homogeneously across the landscape and (ii) the proxy signal is not significantly affected by transport.

As highlighted above and despite large variability, the brGDGT concentrations in soils do not vary systematically with elevation, precipitation, or aspect, and TOC-normalized brGDGT concentrations and brGDGT distributions are invariant with soil depth. The MAT_{GDGT} of river sediments can, therefore, be used to directly trace soil organic matter provenance in the catchments without further correction or weighting.

We assume that in situ production of brGDGTs in trans-Himalayan rivers is negligible given the short transit times and high turbidity of these fluvial systems. Substantial in situ production would bias the reconstructed MAT_{GDGT} and lead to a significant increase of the isomer ratio of brGDGTs (De Jonge, Stadnitskaia, et al., 2014) beyond what is observed in our data set (see Figure S2f). The lapse rate obtained from river sediment MAT_{GDGT} (5.7°C/km, based on mean catchment elevation) agrees with the lapse rate of MAT_{GDGT} from the Himalayan soils (6.4°C/km), further suggesting that soils are the main source of brGDGTs in river sediments.

Given that degradation of organic matter during riverine transport in a headwater system with minimal sediment storage is likely limited (Scheingross et al., 2019) and that soil and river sediment-based lapse rates mentioned above are similar, this implies that brGDGTs in suspended sediments faithfully integrate upstream conditions (Kirkels et al., 2020). It is therefore possible to interpret the fluvial brGDGT signal in terms of the elevational provenance of SOC mobilized in the Central Himalayan catchments. Comparison of the elevation calculated from the MAT_{GDGT} of river suspended sediments against the entire hypsometry of the upstream catchments indicates that soil organic matter is derived from below the mean elevation for most catchments. Since surfaces above 5,000–5,500 m asl are mostly covered by rocky terrain and glaciers with little to no soils, such a discrepancy is expected, and therefore the mean elevation of the soil-covered portion of a catchment serves a better representation of the likely provenance of soil-derived organic matter (difference between Figure 2 and Figure S4). As such, we use the mean soil elevation derived from land cover maps (Jun et al., 2014; Uddin et al., 2015) and from vegetation-covered areas obtained from NDVI maps (Didan, 2015). Both land cover and NDVI maps show a similar hypsometry in the different catchments (Table S3), suggesting that they provide good approximations of the mean elevation of soils in the respective catchments. The coarse resolution of these data sets compared to the elevation data likely induces a small overestimation of soil cover at elevations >5,000 m asl. For the remaining analyses, we use the elevations calculated with the land cover maps.

The elevation provenance inferred from the river-derived MAT_{GDGT} agrees well with the soil-covered average elevation of most catchments (Figure 2). We use this calibrated MAT_{GDGT}-elevation profile together with MAT_{GDGT} values of river sediments to calculate the source elevation of brGDGTs entrained in the riverine suspended load. In Figure 3, this calculated mean elevation for river sediment brGDGTs is compared to the elevation of different land covers as well as the average slope of soil-covered portions of the catchment, binned by elevation.

In most studied catchments, the brGDGT signals in river sediments matches the mean altitude of the total soil-covered catchments (Figure 3). No specific elevation or land cover type dominates the SOC exported by river sediments in these Central Himalayan catchments. This suggests that SOC exported by rivers as particulate organic matter represents an integrated signature of all soil-covered elevations within the catchment and is not derived from specific elevation bands. This observation does not change between smaller drainage basins in the Upper Himalaya and larger basins integrating the Upper Himalaya and the Middle Hills. In addition, our data do not point toward any systematic temporal changes in soil provenance despite marked seasonal and interannual changes in the amount of total sediment and SOC export (Morin et al., 2018). There is furthermore no direct evidence for changes in soil provenance linked to the 2015 Gorkha earthquake-induced landslides which affected the studied catchments to different degrees. Specifically, heavily impacted catchments such as upstream of Barabise or Devighat do not show significant differences compared to unaffected catchments such as upstream of Chame or Besisahar (Roback et al., 2018).

Suspended sediments from the two rivers draining only the Middle Hills (Manahari and Walling) exhibit brGDGT signatures that would suggest that their SOC predominantly derives from an elevation above the average soil-covered elevation (Figure 3). This signal could have been affected by in situ production of GDGTs or could be biased because of the saturation of the MAT_{GDGT} calibration above 22.9°C (De Jonge, Hopmans, et al., 2014). Samples from Chatara and Barabise display brGDGT signals biased toward lower elevations than their mean soil-covered catchment elevation (Figure 3). This observation could be explained by enhanced SOC export from agricultural areas at lower elevations (see sensitivity calculation in the supporting information).

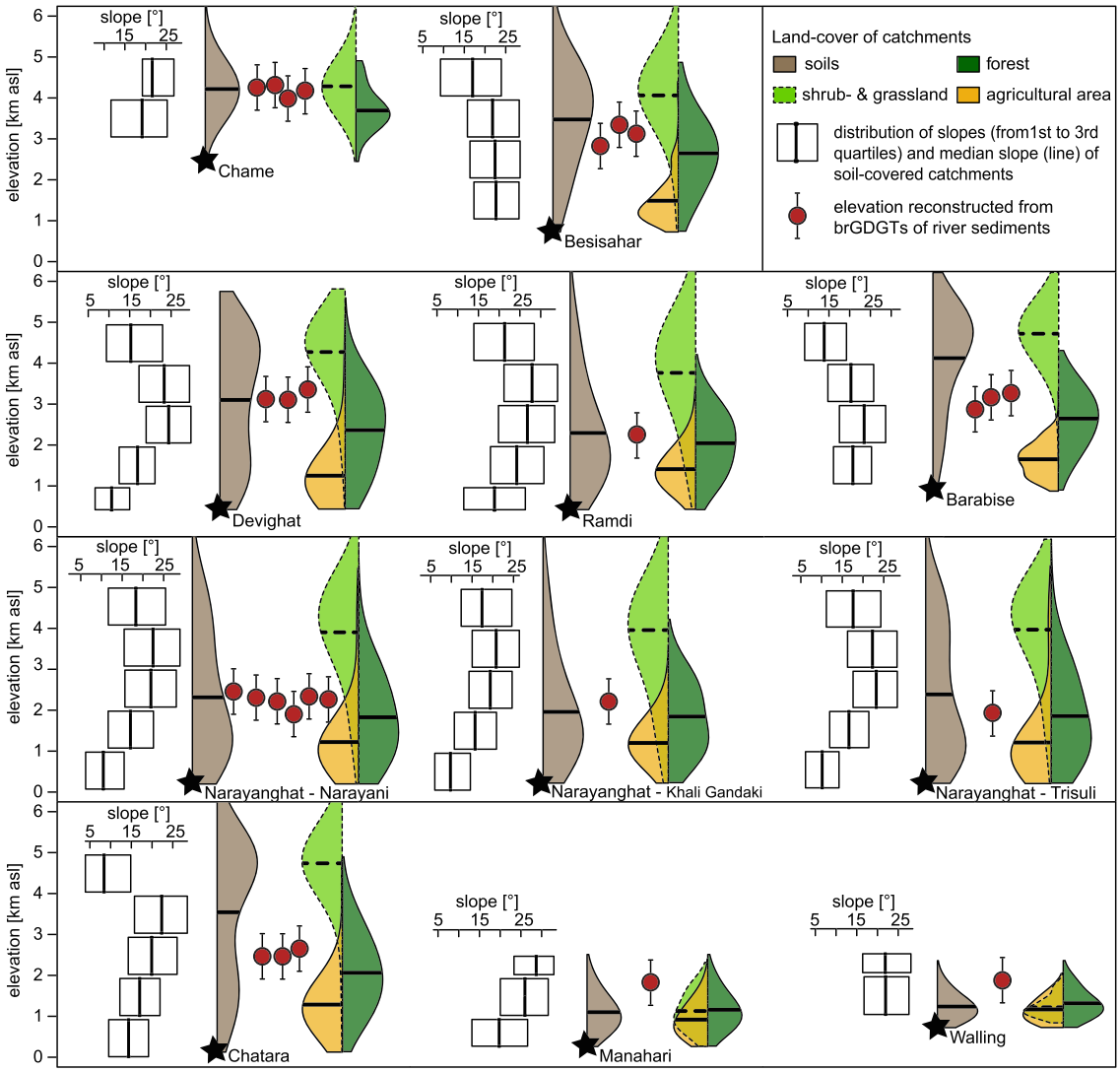

Figure 3. Violin plots showing the elevations of the total soil-covered catchments and of different land covers (shrubland and grassland, forest, and agricultural area). Black lines indicate the mean values; stars are at the sampling site elevation. The slopes of five altitudinal portions of the soil-covered catchments are illustrated with boxplots without whiskers. Red circles show the mean elevation of SOC reflected in river suspended sediments calculated using corresponding MAT_{GDGT} values. Error bars correspond to the confidence interval of the MAT_{GDGT}-elevation calibration.

Soil production and erosion have been linked to landscape steepness (e.g., Heimsath et al., 2012). In most of the studied catchments, hillslope angles are relatively evenly distributed with elevation (i.e., high slopes are not limited to specific elevation bands), making it difficult to identify a clear hillslope control on river brGDGT signatures (Figure 3). The catchments of Barabise and Chatara are exceptions where the highest elevation bands display significantly flatter topography from drainage portions on the Tibetan Plateau. The observed discrepancy between brGDGT signals from Chatara and Barabise and their respective mean soil-covered catchment elevation is therefore likely attributable to a limited SOC supply from the high-elevation, low-angled and arid Tibetan Plateau, as has been suggested earlier (Hoffmann et al., 2016).

4.3. Relative SOC Yields of Different Land Covers

We use a linear inverse modeling approach in order to test the hypothesis of pervasive soil organic matter export across different land covers in the Central Himalaya (see also the supporting information). This model constrains the relative SOC yield from the catchment's main land cover types (forests, shrublands and grasslands, and agricultural areas) that can best explain the measured brGDGT signatures in the river

sediments. For each catchment, the MAT_{GDGT} measured in river sediments is expressed as a linear function of each land cover type's average temperature (calculated from the land cover elevation distribution in the respective catchments), relative surface area, and the unknown SOC yield from a given land cover type. Inverting the resulting set of equations shows that relative to shrublands and grasslands, forests contribute by a factor of ~0.85 (0.26–1.66, q5 to q95 range) and agricultural areas by a factor ~1.56 (1.00–2.10, q5 to q95 range) to SOC yields per unit surface area (uncertainties are propagated from the uncertainty in the elevation-MAT_{GDGT} regression using a Monte Carlo approach). Similar results (forests: 1.99; agricultural areas: 1.30), albeit with greater uncertainty, are obtained for inversions that do not take into account the two small catchments discussed above (Manahari and Walling). The inversion is thus not sensitive to minor differences in SOC yields due to the heterogeneities between the catchments which cause relatively large errors. The inversion would, however, capture orders of magnitude differences in soil erosion rates expected in anthropogenically perturbed systems (Montgomery, 2007; Tarolli & Sofia, 2016). Our results therefore suggests that no specific land cover type significantly dominates SOC export at the scale of the Central Himalaya, as anticipated from the results of Figure 3.

4.4. Implications for Soil Organic Matter Export in the Central Himalaya

The brGDGT signals in rivers of Central Nepal show that soil organic matter entrained in their suspended load is predominantly sourced from the entire soil-mantled catchment in the Central Himalaya with a reduced SOC input from the Tibetan Plateau. The fact that brGDGT distributions in river sediments reflect the average soil-covered elevation irrespective of catchment size or mean elevation further demonstrates that brGDGTs are sourced from the entire elevation range of soil cover in the catchment. These results therefore suggest that SOC export in Himalayan catchments is both pervasive and uniform and is not restricted to certain elevations or land cover types. SOC inputs due to deforestation and agriculture in the Middle Hills are therefore either negligible in comparison to overall background soil erosion processes or these erosional effects are balanced out by OC inputs through naturally enhanced soil erosion in the steeper Upper Himalaya (Montgomery, 2007; Tarolli & Sofia, 2016; West et al., 2015). While mass wasting processes in the Upper Himalaya lead to high erosion rates (Marc et al., 2019), bedrock landsliding probably mobilizes a relatively low proportion of soil organic matter (Morin et al., 2018). This implies that even if topography, land cover, erosion rates, and annual precipitation rates are very different in the Upper Himalaya and the Nepalese Middle Hills, riverine SOC input must be fairly evenly distributed in order to not induce any significant elevation bias in brGDGT signals over the study area.

Other studies in the Himalaya have pointed at a predominant mobilization of organic matter from the southern flank of the Himalaya (Hoffmann et al., 2016). The latter study focused on leaf-wax lipid biomarkers, which mainly trace vascular plant inputs. We find similar results for the catchments of Chatara and Barabise; however, our data set as a whole suggests a more widespread provenance of SOC. This possible decoupling of the brGDGT and plant-wax lipid provenance signals in river sediments may be attributed to broader altitudinal distribution of SOC compared to vascular plants OC in the Himalaya and/or to a more rapid remineralization of plant-wax lipids as it has been observed in the Andes (Feakins et al., 2018; Kirkels et al., 2020).

4.5. Implications for the Integrative Nature of brGDGTs Signatures in River Sediments

The signature of soil organic matter originating from all soil-covered elevations is found at the outlets of most Central Himalayan rivers. Trans-Himalayan rivers thus integrate the molecular signal from the entire soil-covered catchment, implying minimal loss of brGDGTs during transport. This is similar to observations from Andean headwaters (Kirkels et al., 2020) but contrasts with studies from larger river systems as the Danube (Freymond et al., 2017) or the Yangtze River (Li et al., 2015). The high turbidity and short transit times of sediments and associated organic matter in mountainous rivers such as in the Central Himalaya transfer soil brGDGT signals with minimal apparent degradation. Thus, brGDGT distributions carried by suspended sediments of mountainous headwater rivers serve as reliable proxies of environmental conditions such as elevation or temperature of entire catchments. The downstream evolution of these brGDGT signals in the Gangetic floodplain remains to be studied, but long sediment transfer times and extensive storage may cause overprinting of the headwater signals as is the case for a significant fraction of the exported organic matter (Galy et al., 2008).

5. Conclusions

The MAT_{GDGT} in soils along an altitudinal transect in the Central Himalaya follow the adiabatic temperature change with altitude and therefore correlate with the elevation of the sampling location. Due to the absence of any systematic relation between soil brGDGT concentrations and elevation, it is possible to directly use the MAT_{GDGT} of soil brGDGTs as an elevation proxy. This soil MAT_{GDGT}-elevation calibration is then used to trace the elevational provenance of SOC in suspended sediments of Central Himalayan rivers in order to identify possible zones of preferential soil organic matter mobilization.

Calculated MAT_{GDGT} values of surface soils using a global calibration closely follow the expected temperature of the sampling location. This highlights the possibility of using brGDGTs for reconstruction of paleoenvironmental conditions in the Central Himalaya.

Elevations calculated based on the MAT_{GDGT} of river sediments reflect the average elevation of the soil cover found in most catchments. This implies that riverine SOC export is a uniform and pervasive process in the Central Himalaya, occurring over the entire range of elevations mantled by soil, whereas the SOC export efficiency on the Tibetan Plateau is probably substantially lower. Inversion of the brGDGT signals suggests no significant difference in relative SOC yield from different land covers. Possible enhanced soil organic matter mobilization due to anthropogenic activities such as agriculture or deforestation are therefore subordinate to soil mobilization by active natural erosion processes at higher elevations.

Data Availability Statement

The data used in this paper are available for download at: https://www.research-collection.ethz.ch/handle/20.500.11850/431464.

Acknowledgments
This study was funded by Grant No. 200021_166067 from the Swiss National Science Foundation. We thank D. Montluçon for lab work support and C. De Jonge for helpful discussions. We are grateful to J. J. Baronas and an anonymous reviewer for their insightful comments that helped to improve the manuscript. We also thank R. Cory for the efficient editorial handling.

References

Alewell, C., Meusburger, K., Brodbeck, M., & Bänninger, D. (2008). Methods to describe and predict soil erosion in mountain regions. *Landscape and Urban Planning*, *88*(2–4), 46–53. https://doi.org/10.1016/j.landurbplan.2008.08.007

Bai, Y., Chen, C., Xu, Q., & Fang, X. (2018). Paleoaltimetry potentiality of branched GDGTs from southern Tibet. *Geochemistry, Geophysics, Geosystems*, *19*, 551–564. https://doi.org/10.1002/2017GC007122

Berhe, A. A., Harden, J. W., Torn, M. S., Kleber, M., Burton, S. D., & Harte, J. (2012). Persistence of soil organic matter in eroding versus depositional landform positions. *Journal of Geophysical Research*, *117*, G02019. https://doi.org/10.1029/2011JG001790

Burbank, D. W., Blythe, A. E., Putkonen, J. L., Pratt-Situala, B. A., Gabet, E. J., Oskin, M. E., et al. (2003). Decoupling of erosion and climate in the Himalaya. *Nature*, *426*(6967), 652–655. Retrieved from. https://doi.org/10.1038/nature02187

Cao, M., Rueda, G., Rivas-Ruiz, P., Carmen, M., Henriksen, M., Vegas-vilarrúbia, T., & Rosell-melé, A. (2018). Organic geochemistry branched GDGT variability in sediments and soils from catchments with marked temperature seasonality. *Organic Geochemistry*, *122*, 98–114. https://doi.org/10.1016/j.orggeochem.2018.05.007

De Jonge, C., Hopmans, E. C., Zell, C. I., Kim, J. H., Schouten, S., & Sinninghe Damsté, J. S. (2014). Occurrence and abundance of 6-methyl branched glycerol dialkyl glycerol tetraethers in soils: Implications for palaeoclimate reconstruction. *Geochimica et Cosmochimica Acta*, *141*, 97–112. https://doi.org/10.1016/j.gca.2014.06.013

De Jonge, C., Stadnitskaia, A., Hopmans, E. C., Cherkashov, G., Fedotov, A., & Sinninghe Damsté, J. S. (2014). In situ produced branched glycerol dialkyl glycerol tetraethers in suspended particulate matter from the Yenisei River, eastern Siberia. *Geochimica et Cosmochimica Acta*, *125*, 476–491. https://doi.org/10.1016/j.gca.2013.10.031

Deng, L., Jia, G., Jin, C., & Li, S. (2016). Warm season bias of branched GDGT temperature estimates causes underestimation of altitudinal lapse rate. *Organic Geochemistry*, *96*, 11–17. https://doi.org/10.1016/j.orggeochem.2016.03.004

Didan, K. (2015). MOD13Q1 MODIS/Terra vegetation indices 16-Day L3 Global 250m SIN Grid V006. *NASA EOSDIS LP DAAC*.

Doetterl, S., Berhe, A. A., Nadeu, E., Wang, Z., Sommer, M., & Fiener, P. (2016). Erosion, deposition and soil carbon: A review of process-level controls, experimental tools and models to address C cycling in dynamic landscapes. *Earth-Science Reviews*, *154*, 102–122. https://doi.org/10.1016/j.earscirev.2015.12.005

Eckholm, E. P. (1975). The deterioration of mountain environments. *Science*, *189*(4205), 764–770. https://doi.org/10.1126/science.189.4205.764

Ernst, N., Peterse, F., Breitenbach, S. F. M., Syiemlieh, H. J., & Eglinton, T. I. (2013). Biomarkers record environmental changes along an altitudinal transect in the wettest place on Earth. *Organic Geochemistry*, *60*, 93–99. https://doi.org/10.1016/j.orggeochem.2013.05.004

Feakins, S. J., Wu, M. S., Ponton, C., Galy, V., & West, A. J. (2018). Dual isotope evidence for sedimentary integration of plant wax biomarkers across an Andes-Amazon elevation transect. *Geochimica et Cosmochimica Acta*, *242*, 64–81. https://doi.org/10.1016/j.gca.2018.09.007

France-Lanord, C., & Derry, L. A. (1997). Organic carbon burial forcing of the carbon cycle from Himalayan erosion. *Nature*, *390*(6655), 65–67. https://doi.org/10.1038/36324

Freymond, C. V., Lupker, M., Peterse, F., Haghipour, N., Wacker, L., Filip, F., et al. (2018). Constraining instantaneous fluxes and integrated compositions of fluvially discharged organic matter. *Geochemistry, Geophysics, Geosystems*, *19*, 2453–2462. https://doi.org/10.1029/2018GC007539

Freymond, C. V., Peterse, F., Fischer, L. V., Filip, F., Giosan, L., & Eglinton, T. I. (2017). Branched GDGT signals in fluvial sediments of the Danube River basin: Method comparison and longitudinal evolution. *Organic Geochemistry*, *105*, 37–38. https://doi.org/10.1016/j.orggeochem.2017.01.001

Gabet, E. J., Burbank, D. W., Pratt-Sitaula, B., Putkonen, J., & Bookhagen, B. (2008). Modern erosion rates in the High Himalayas of Nepal. *Earth and Planetary Science Letters*, *267*(3–4), 482–494. https://doi.org/10.1016/j.epsl.2007.11.059

Galy, V., France-Lanord, C., & Lartiges, B. (2008). Loading and fate of particulate organic carbon from the Himalaya to the Ganga-Brahmaputra delta. *Geochimica et Cosmochimica Acta*, *72*(7), 1767–1787. https://doi.org/10.1016/j.gca.2008.01.027

Galy, V., Peucker-Ehrenbrink, B., & Eglinton, T. (2015). Global carbon export from the terrestrial biosphere controlled by erosion. *Nature*, *521*(7551), 204–207. https://doi.org/10.1038/nature14400

Gardner, R. A. M., & Gerrard, A. J. (2003). Runoff and soil erosion on cultivated rainfed terraces in the Middle Hills of Nepal. *Applied Geography*, *23*(1), 23–45. https://doi.org/10.1016/S0143-6228(02)00069-3

Heimsath, A. M., DiBiase, R. A., & Whipple, K. X. (2012). Soil production limits and the transition to bedrock-dominated landscapes. *Nature Geoscience*, *5*(3), 210–214. https://doi.org/10.1038/ngeo1380

HMG (1995). His Majesty's Government of Nepal. In *Climatological Records of Nepal 1987–1990* (Chap. 1). Kathmandu: Department of Hydrology and Meteorology

Hoffmann, B., Feakins, S. J., Bookhagen, B., Olen, S. M., Adhikari, D. P., Mainali, J., & Sachse, D. (2016). Climatic and geomorphic drivers of plant organic matter transport in the Arun River, E Nepal. *Earth and Planetary Science Letters*, *452*, 104–114. https://doi.org/10.1016/j.epsl.2016.07.008

Hopmans, E. C., Schouten, S., & Sinninghe Damsté, J. S. (2016). The effect of improved chromatography on GDGT-based palaeoproxies. *Organic Geochemistry*, *93*, 1–6. https://doi.org/10.1016/j.orggeochem.2015.12.006

Huguet, C., Hopmans, E. C., Febo-Ayala, W., Thompson, D. H., Sinninghe Damsté, J. S., & Schouten, S. (2006). An improved method to determine the absolute abundance of glycerol dibiphytanyl glycerol tetraether lipids. *Organic Geochemistry*, *37*(9), 1036–1041. https://doi.org/10.1016/j.orggeochem.2006.05.008

Jacinthe, P. A., & Lal, R. (2001). A mass balance approach to assess carbon dioxide evolution during erosional events. *Land Degradation and Development*, *12*(4), 329–339. https://doi.org/10.1002/ldr.454

Jobbagy, E. G., & Jackson, R. B. (2000). The vertical distribution of soil organic carbon and its relation to climate and vegetation. *Ecological Applications*, *10*(2), 423–436. https://doi.org/10.1890/1051-0761(2000)010[0423:TVDOSO]2.0.CO;2

Jun, C., Ban, Y., & Li, S. (2014). Open access to Earth land-cover map. *Nature*, *514*(7523), 434. https://doi.org/10.1038/514434c

Kirkels, F. M. S. A., Ponton, C., Galy, V., West, A. J., Feakins, S. J., & Peterse, F. (2020). From Andes to Amazon: Assessing branched tetraether lipids as tracers for soil organic carbon in the Madre de Dios River system. *Journal of Geophysical Research: Biogeosciences*, *125*, e2019JG005270. https://doi.org/10.1029/2019JG005270

Li, Z., Peterse, F., Wu, Y., Bao, H., Eglinton, T. I., & Zhang, J. (2015). Sources of organic matter in Changjiang (Yangtze River) bed sediments: Preliminary insights from organic geochemical proxies. *Organic Geochemistry*, *85*, 11–21. https://doi.org/10.1016/j.orggeochem.2015.04.006

Ludwig, W., Probst, J. L., & Kempe, S. (1996). Predicting the oceanic input of organic carbon by continental erosion. *Global Biogeochemical Cycles*, *10*(1), 23–41. https://doi.org/10.1029/95GB02925

Marc, O., Behling, R., Andermann, C., Turowski, J. M., Illien, L., Roessner, S., & Hovius, N. (2019). Long-term erosion of the Nepal Himalayas by bedrock landsliding: The role of monsoons, earthquakes and giant landslides. *Earth Surface Dynamics*, *7*(1), 107–128. https://doi.org/10.5194/esurf-7-107-2019

Montgomery, D. R. (2007). Soil erosion and agricultural sustainability. *Proceedings of the National Academy of Sciences*, *104*(33), 13,268–13,272. https://doi.org/10.1073/pnas.0611508104

Morin, G. P., Lavé, J., France-Lanord, C., Rigaudier, T., Gajurel, A. P., & Sinha, R. (2018). Annual sediment transport dynamics in the Narayani Basin, Central Nepal: Assessing the impacts of erosion processes in the annual sediment budget. *Journal of Geophysical Research: Earth Surface*, *123*, 2341–2376. https://doi.org/10.1029/2017JF004460

Patton, N. R., Lohse, K. A., Seyfried, M. S., Godsey, S. E., & Parsons, S. B. (2019). Topographic controls of soil organic carbon on soil-mantled landscapes. *Scientific Reports*, *9*(1), 1–15. https://doi.org/10.1038/s41598-019-42556-5

Peterse, F., Van Der Meer, M. T. J., Schouten, S., Jia, G., Ossebaar, J., Blokker, J., & Sinninghe Damsté, J. S. (2009). Assessment of soil n-alkane δd and branched tetraether membrane lipid distributions as tools for paleoelevation reconstruction. *Biogeosciences*, *6*(12), 2799–2807. https://doi.org/10.5194/bg-6-2799-2009

Putkonen, J. K. (2004). Continuous snow and rain data at 500 to 4400 m altitude near Annapurna, Nepal, 1999-2001. *Arctic, Antarctic, and Alpine Research*, *36*(2), 244–248. https://doi.org/10.1657/1523-0430(2004)036[0244:CSARDA]2.0.CO;2

Roback, K., Clark, M. K., West, A. J., Zekkos, D., Li, G., Gallen, S. F., et al. (2018). The size, distribution, and mobility of landslides caused by the 2015 Mw7.8 Gorkha earthquake, Nepal. *Geomorphology*, *301*, 121–138. https://doi.org/10.1016/j.geomorph.2017.01.030

Scharlemann, J. P. W., Tanner, E. V. J., Hiederer, R., & Kapos, V. (2014). Global soil carbon: Understanding and managing the largest terrestrial carbon pool. *Carbon Management*, *5*(1), 81–91. https://doi.org/10.4155/cmt.13.77

Scheingross, J. S., Hovius, N., Dellinger, M., Hilton, R. G., Repasch, M., Sachse, D., et al. (2019). Preservation of organic carbon during active fluvial transport and particle abrasion. *Geology*, *47*(10), 958–962. https://doi.org/10.1130/G46442.1

Schlesinger, W. H. (1995). Soil respiration and changes in soil carbon stocks. In *Biotic feedbacks in the global climatic system: Will the warming feed the warming* (pp. 159–168). Oxford, UK: Oxford University Press.

Schouten, S., Hopmans, E. C., & Sinninghe Damsté, J. S. (2013). The organic geochemistry of glycerol dialkyl glycerol tetraether lipids: A review. *Organic Geochemistry*, *54*, 19–61. https://doi.org/10.1016/j.orggeochem.2012.09.006

Semwal, R. L., Nautiyal, S., Sen, K. K., Rana, U., Maikhuri, R. K., Rao, K. S., & Saxena, K. G. (2004). Patterns and ecological implications of agricultural land-use changes: A case study from central Himalaya, India. *Agriculture, Ecosystems and Environment*, *102*(1), 81–92. https://doi.org/10.1016/S0167-8809(03)00228-7

Sinninghe Damasté, J. S., Ossebaar, J., Schouten, S., & Verschuren, D. (2012). Distribution of tetraether lipids in the 25-ka sedimentary record of Lake Challa: Extracting reliable TEX 86 and MBT/CBT palaeotemperatures from an equatorial African lake. *Quaternary Science Reviews*, *50*, 43–54. https://doi.org/10.1016/j.quascirev.2012.07.001

Smith, S. V., Renwick, W. H., Buddemeier, R. W., & Crossland, C. J. (2001). Budgets of soil erosion and deposition for sediments and sedimentary organic carbon across the posited across the United States. *Global Biogeochemical Cycles*, *15*(3), 697–707. https://doi.org/10.1029/2000GB001341

Stallard, R. F. (1998). Terrestrial sedimentation and the carbon cycle: Coupling weathering and erosion to carbon burial. *Water Resources*, *12*(2), 231–257.

Stockmann, U., Adams, M. A., Crawford, J. W., Field, D. J., Henakaarchchi, N., Jenkins, M., et al. (2013). The knowns, known unknowns and unknowns of sequestration of soil organic carbon. *Agriculture, Ecosystems and Environment*, *164*, 80–99. https://doi.org/10.1016/j.agee.2012.10.001

Tarolli, P., & Sofia, G. (2016). Human topographic signatures and derived geomorphic processes across landscapes. *Geomorphology*, *255*, 140–161. https://doi.org/10.1016/j.geomorph.2015.12.007

Uddin, K., Shrestha, H. L., Murthy, M. S. R., Bajracharya, B., Shrestha, B., Gilani, H., et al. (2015). Development of 2010 national land cover database for the Nepal. *Journal of Environmental Management*, *148*, 82–90. https://doi.org/10.1016/j.jenvman.2014.07.047

Upadhayay, H. R., Smith, H. G., Griepentrog, M., Bodé, S., Man, R., Blake, W., et al. (2018). Community managed forests dominate the catchment sediment cascade in the mid-hills of Nepal: A compound-specific stable isotope analysis. *Science of the Total Environment*, *637–638*, 306–317. https://doi.org/10.1016/j.scitotenv.2018.04.394

Wang, Z., Hoffmann, T., Six, J., Kaplan, J. O., Govers, G., Doetterl, S., & Van Oost, K. (2017). Human-induced erosion has offset one-third of carbon emissions from land cover change. *Nature Climate Change*, *7*(5), 345–349. https://doi.org/10.1038/nclimate3263

Wasson, R. J., Juyal, N., Jaiswal, M., McCulloch, M., Sarin, M. M., Jain, V., et al. (2008). The mountain-lowland debate: Deforestation and sediment transport in the upper Ganga catchment. *Journal of Environmental Management*, *88*(1), 53–61. https://doi.org/10.1016/j.jenvman.2007.01.046

Weijers, J. W. H., Schefuß, E., Schouten, S., & Damsté, J. S. S. (2007). Evolution of tropical Africa over the last deglaciation. *Science*, *315*(5819), 1701–1704. https://doi.org/10.1126/science.1138131

Weijers, J. W. H., Schouten, S., van den Donker, J. C., Hopmans, E. C., & Sinninghe Damsté, J. S. (2007). Environmental controls on bacterial tetraether membrane lipid distribution in soils. *Geochimica et Cosmochimica Acta*, *71*(3), 703–713. https://doi.org/10.1016/j.gca.2006.10.003

West, A. J., Arnold, M., Aumaître, G., Bourlès, D. L., Keddadouche, K., Bickle, M., & Ojha, T. (2015). High natural erosion rates are the backdrop for present-day soil erosion in the agricultural Middle Hills of Nepal. *Earth Surface Dynamics*, *3*(3), 363–387. https://doi.org/10.5194/esurf-3-363-2015

Yoo, K., Amundson, R., Heimsath, A. M., & Dietrich, W. E. (2006). Spatial patterns of soil organic carbon on hillslopes: Integrating geomorphic processes and the biological C cycle. *Geoderma*, *130*(1–2), 47–65. https://doi.org/10.1016/j.geoderma.2005.01.008

Yue, Y., Ni, J., Ciais, P., Piao, S., Wang, T., Huang, M., et al. (2016). Lateral transport of soil carbon and land-atmosphere CO_2 flux induced by water erosion in China. *Proceedings of the National Academy of Sciences of the United States of America*, *113*(24), 6617–6622. https://doi.org/10.1073/pnas.1523358113